https://dx.doi.org/10.22161/ijaers.78.15 *ISSN: 2349-6495(P) | 2456-1908(O)*

The correct choice among welding wires ER70S-2, ER70S-3 and ER70S-6, according to the oxidation level of base metal

André de Albuquerque Vicente[1,2], Peter Aloysius D'silva[2], Rajesh Babu[2], Italo Leonardo dos Santos[2], Renato Rodrigues de Aguiar[2], Tiago Felipe de Abreu Santos[3]

[1]Department of Chemical Engineering, Universidade de São Paulo, Rua do Lago,250, Cidade Universitária, São Paulo, SP, Brazil;
[2]ESAB Middle East & Africa,Plot No. S20134, Jebel Ali Free Zone (South), PO Box 8964, Dubai, United Arab Emirates;
[3]Department of Mechanical Engineering, Universidade Federal de Pernambuco, Av. da Arquitetura, s/n, Cidade Universitária, Recife, PE, Brazil.

***Abstract*—** *According to AWS 5.18, the all weld metals produced with filler metals ER70S-2, ER70S-3 and ER70S-6 through GTAW should present the same minimum values in tensile tests, as follows, minimum yield strength 400 MPa, minimum tensile strength 480 MPa and minimum elongation 22%. The impact test requirements to the all weld metals produced with filler metals ER70S-2, ER70S-3 and ER70S-6 should present 27 J as the minimum average impact strength at -29 °C to ER70S-2 and ER70S-6, and at -18 °C to ER70S-3. Although the mechanical properties of the all weld metals produced using these three welding electrodes are quite similar, their chemical compositions are different specially in the contents of deoxidizing elements like Zr, Al, Ti, Si and Mn. The contents of deoxidizing elements are lower in ER70S-3, intermediate in ER70S-6 and higher in ER70S-2. Electrodes and rods of the ER70S-2 classification are primarily used for single-pass welding of killed, semi-killed, and rimmed steels, but may be used for some multipass applications. Due to the added deoxidants Zr, Al and Ti in the chemical composition of ER70S-2, this filler metal can be used for welding steels that have a rusty or dirty surface,with a possible sacrifice of weld quality depending on the condition of the surface. A detailed study to compare the performance of filler metals ER70S-2, ER70S-3 and ER70S-6 was conducted through GTAW bead on plate coupons using the three different electrodes on bright polished and rusty plates. The performance of the electrodes was studied through GTAW groove test weld assembly with and without purging gas. The results showed that, although ER70S-2 presented the best performance among the three welding wires tested in bead on plate in rusty plates, welding groove joints without purging gas using this welding electrode is practically unviable though GTAW. Fluid flow in the weld pool determines GTAW weld pool shape. The force driving the fluid flow is surface tension gradient. This is called Marangoni convection. Due to the higher contents of deoxidants in the chemical composition of ER70S-2, the weld pool produced using this filler wire is strongly deoxidized and the result is that when the area under the arc is heated up, the surface tension drops in the center of the weld pool and the direction of the fluid flow is from the center towards the edges of the pool. The results suggest that the change in the fluid movement due to deoxidation of the weld pool, causes slag to be trapped between base metal and weld pool.*

Keywords*— *ER70S-2; ER70S-3; ER70S-6, Slag formation, Marangoni effect.

I. INTRODUCTION

The Ellingham diagram is used to predict the equilibrium temperature between a metal, its oxide, and oxygen, and by extension, reactions of a metal with sulfur, nitrogen, and other non-metals. The analysis is thermodynamic in nature and ignores reaction kinetics. Thus, processes that are predicted to be favorable by the Ellingham diagram can still be slow. Figure 1 shows the Ellingham diagram for oxide formation. It is observed that aluminum is oxidized preferentially to titanium, silicon, manganese and iron due to the fact that Gibbs free energy of alumina

https://dx.doi.org/10.22161/ijaers.78.15 *ISSN: 2349-6495(P) | 2456-1908(O)*

formation (Al_2O_3) is more negative than Gibbs free energy of rutile formation (TiO_2), silica formation (SiO_2),manganese (II) oxide (MnO) and iron oxides (FeO, Fe_3O_4 and Fe_2O_3).**[1-7]**

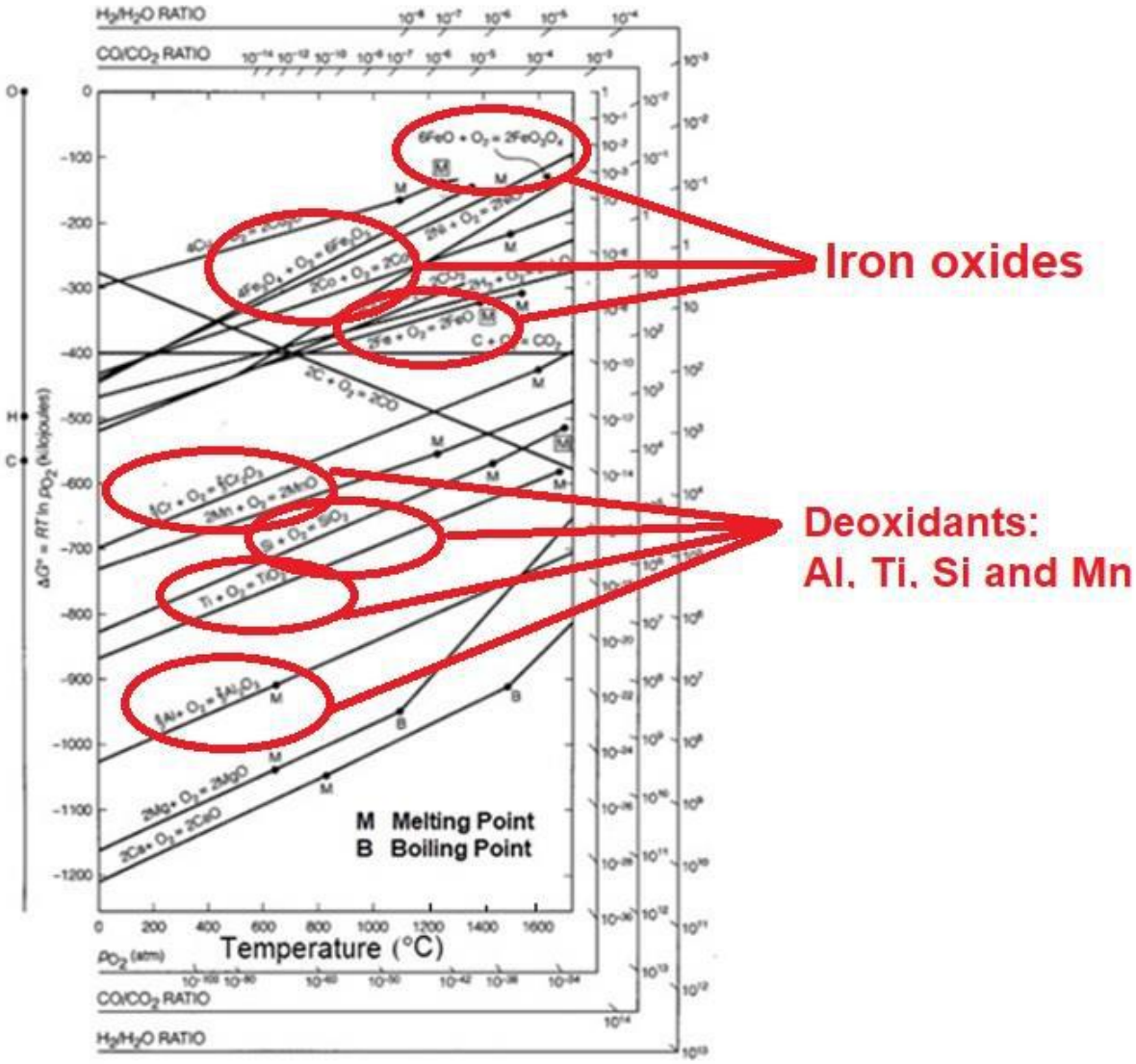

Fig.1: Ellingham diagram of oxides formation. [1,7]

Figure 2 presents the standard free Gibbs Energy (ΔG^o) of the reactions for the formation of oxides, sulfides, nitrides and carbides at 1723 K. It is important to observe that zirconium presents higher affinity with oxygen, sulfur, nitrides and carbides when compared to the other deoxidants aluminum, titanium, silicon and manganese.

https://dx.doi.org/10.22161/ijaers.78.15 *ISSN: 2349-6495(P) | 2456-1908(O)*

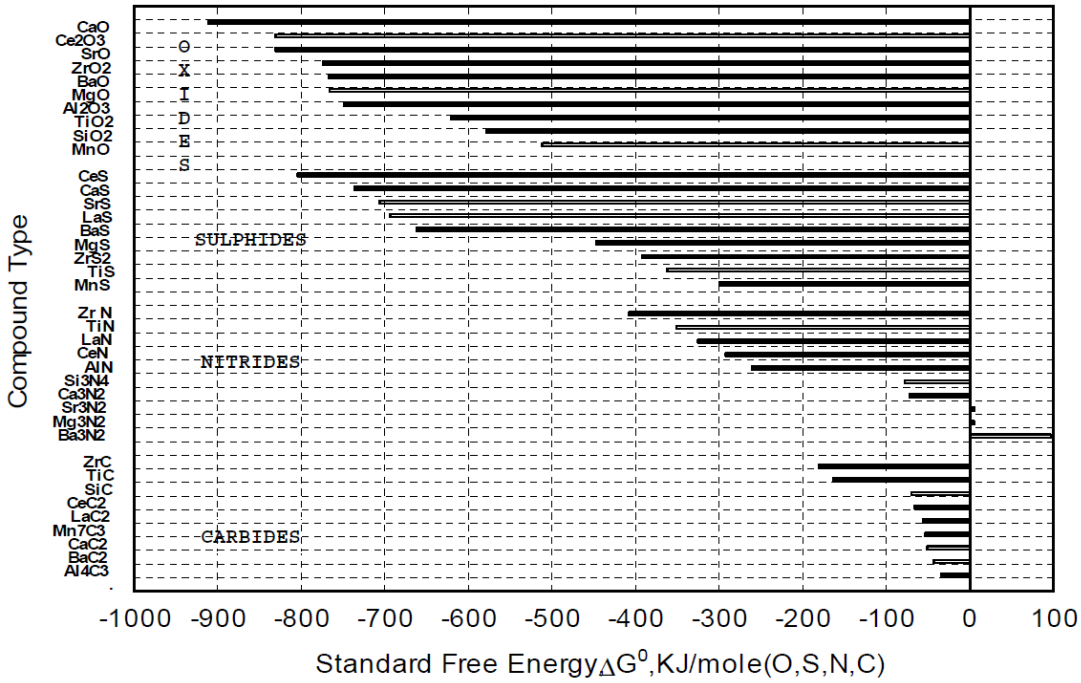

Fig.2: *Standard free Gibbs Energy (ΔG^o) of the reactions for the formation of oxides, sulfides, nitrides and carbides at 1723 K.* ***[8]***

Although the mechanical properties of the all weld metals produced using ER70S-2, ER70S-3 and ER70S-6 welding electrodes are quite similar, their chemical compositions are different specially in the contents of deoxidant elements like Zr, Al, Ti, Si and Mn. The contents of deoxidizing elements are lower in ER70S-3, intermediate in ER70S-6 and higher in ER70S-2.

This information suggests that all weld metals produced using ER70S-2 tends to present lower oxygen contents than those produced using ER70S-6 and ER70S-3, respectively, when welding base metals with similar oxygen concentrations.

In this context, a deeply understanding of the Marangoni effect, looks to be very important to do the correct choice among welding wires ER70S-2, ER70S-3 and ER70S-6, according to the oxidation level of base metal.

The Marangoni effect is the mass transfer along an interface between two fluids due to the surface tension gradient. In the case of temperature dependence this phenomenon may be called thermo-capillary convection.**[9-12}**

Since a liquid with a high surface tension pulls more strongly on the surrounding liquid than one with a low surface tension,the presence of a gradient in surface tension will naturally cause the liquid to flow away from regions of low surface tension. The surface tension gradient can be caused by concentration gradient or by a temperature gradient when surface tension is a function of temperature.**[9-12]**

Fluid flow in the weld pool determines GTAW weld pool shape and the force driving the fluid flow is surface tension gradient. This is called Marangoni convection.

Pure metals (and low sulfur materials) have a negative temperature coefficient of surface tension. When the area under the arc is heated up, the surface tension drops in the center of the weld pool and the direction of the fluid flow is from the center towards the edges of the pool. **[9-12]**

When sulfur, oxygen, selenium, or other surface-active elements are introduced to the weld pool at very low levels they cause the surface tension to rise with an increase in temperature. In this case, the direction of fluid flow is from the outside of the pool, where the surface tension is lower, towards the center, thus increasing penetration. **[9-13]**

Figure 3 presents the effect of variation of surface tension with temperature when there is presence of “surface active” elements in the weld pool.

https://dx.doi.org/10.22161/ijaers.78.15 ISSN: 2349-6495(P) | 2456-1908(O)

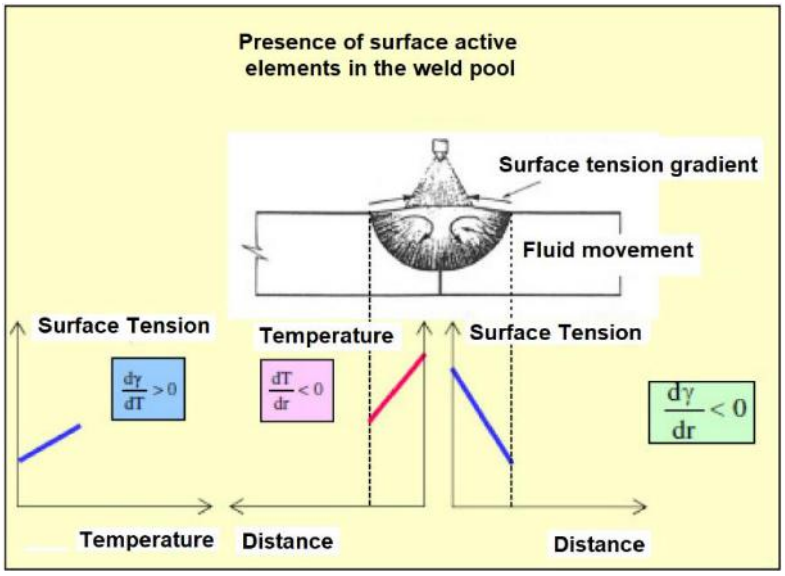

:

Fig.3: Effect of variation of surface tension with temperature when there is presence of "surface active" elements in the weld pool. [9]

Figure 4 presents the effect of variation of surface tension with temperature when there is absence of "surface active" elements in the weld pool.

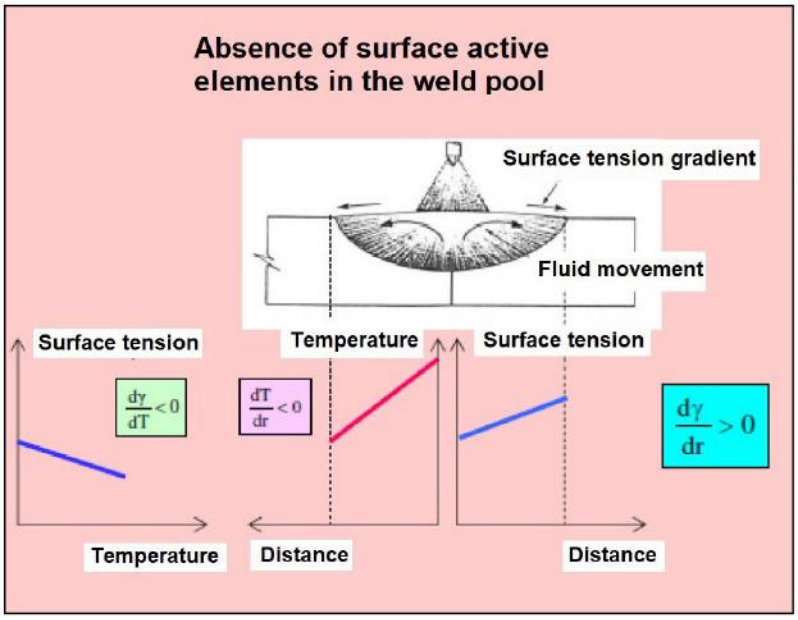

Fig.4: Effect of variation of surface tension with temperature when there is absence of "surface active" elements in the weld pool. [9]

Among the "surface active elements", oxygen can be added or reduced into the weld metal during welding. Alloying elements like silicon and manganese, which are present in the base metal and the wire, have a high affinity to react with oxygen and form silicon oxide and manganese oxide. These oxides accumulate on the surface of the weld pool and form slag. As these slags float on the weld pool surface, the weld pool flow pattern can govern the slag

https://dx.doi.org/10.22161/ijaers.78.15 ISSN: 2349-6495(P) | 2456-1908(O)

formation location. Besides, the slag formation location can also give an indication of the weld pool flow pattern. The slags have an adverse effect on the weld quality.**[12, 13]**

II. EXPERIMENTAL

A detailed study to compare the performance of filler metals ER70S-2, ER70S-3 and ER70S-6, all 2.4 mm diameter, was conducted through GTAW bead on plate coupons using the three different electrodes on bright polished and rusty plates of ASTM A36 150 X 50 X 8 mm.

All the "bead on plate" samples were welded using 99.99% Ar as the shielding gas, 160 A, 14 V and travel speed of 80 mm/minute.

To accelerate rust formation, 3 plates were wet and left at the sun for 8 h in air.

Fig.5: Bright polished and rusty plates of ASTM A36 150 X 50 X 8 mm

The performance of the electrodes was then studied through GTAW groove test weld assembly to allow welding of the root pass with and without purging gas. The plates are of ASTM A36 250 X 50 X 8 mm and the V groove is 60°.

Fig.6: GTAW groove test weld assembly to allow welding with and without purging gas.

The purging gas, when used, was 99.99% Ar. All the "groove test" samples were welded using 99.99% Ar as the shielding gas, 115 A, 11 V and travel speed of 40 mm/minute.

Chemical analyzes were carried out in all samples by means of an optical emission spectrometer, according to ASTM E 1086-08. **[14]**

Afterwards, the conventional manual polishing was applied using water slicks (100, 240, 320, 400, 600 and 1000 mesh) in order to standardize the surface finish of the samples. Afterwards, a cloth polishing with 9, 3 and 1 µm diamond abrasive paste was carried out in this sequence. The etching solution used was Nital.

III. RESULTS AND DISCUSSION

Figures 7 presents the bead on plate coupons using the three different electrodes on bright polished and rusty plates of ASTM A36 150 X 50 X 8 mm.

https://dx.doi.org/10.22161/ijaers.78.15 ISSN: 2349-6495(P) | 2456-1908(O)

Bead on plate (Bright)

a) 

b) 

Bead on plate (Rusty)

c) 
d) 

Fig.7: Bead on plate coupons using the three different electrodes on bright polished (a and b) and rusty plates (c and d) of ASTM A36 150 X 50 X 8 mm

The bead on plate tests showed very interesting results. For the bright plates there was almost no slag formation, although, for the rusty plates there was slag formation for the three different electrodes.

In the case of the bright plates, all the three filler metals presented similar good weldability.

Nonetheless, it is important to emphasize that in the case of rusty plates, the three filler metals presented different performances. The ER70S-3 presented bad weldability once a thin layer of slag was formed on the surface of the bead, and some porosity appeared on the surface, as well. The ER70S-6 presented better weldability than that observed to the ER70S-3, and the slag tended to concentrate on the top of the bead and there was no apparent porosity. The ER70S-2 presented very good weldability and the slag tended to concentrate in the fusion line with the base metal. The bead showed very good wettability and low penetration.

Figure 8 shows the macrographs of the sections of the "bead on plate" coupons produced with filler metals ER70S-2, ER70S-3 and ER70S-6 on the rusty plates.

https://dx.doi.org/10.22161/ijaers.78.15 *ISSN: 2349-6495(P) | 2456-1908(O)*

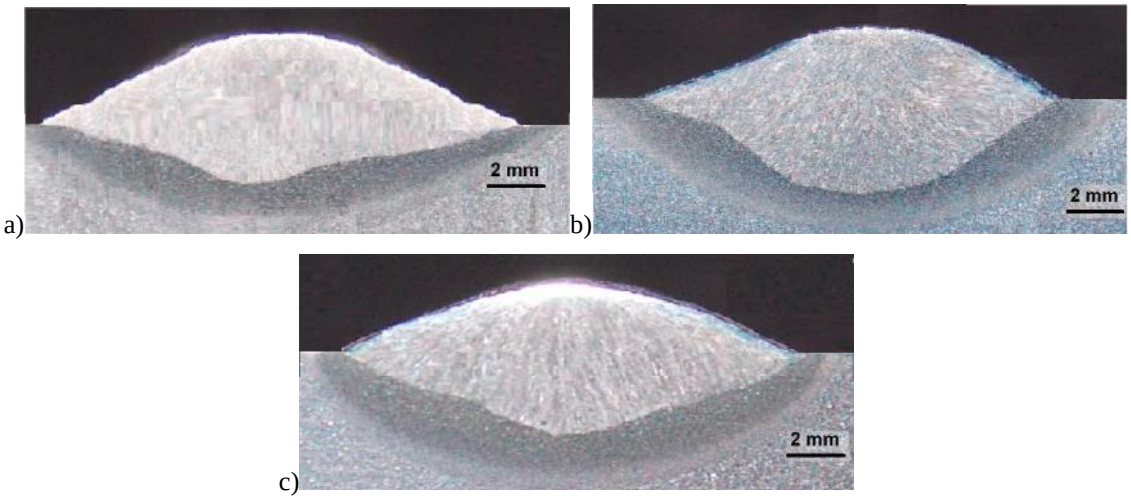

Fig.8: Macrographs of the sections of the "bead on plate" coupons produced with filler metals a) ER70S-2, b) ER70S-3 and c) ER70S-6.

The higher content of deoxidants on the chemical composition of ER70S-2 leads to a lower content of oxygen in the welding pool, resulting in lower penetration and wider bead. The lower content of deoxidants on the chemical composition of ER70S-3 leads to a higher content of oxygen in the welding pool, and consequently, higher penetration and narrower bead.

Figure 9 presents a model to explain the increasing of penetration and decreasing of the bead width as a function of the oxygen content of the weld pool in "bead on plate" deposits through GTAW, according to the content of oxygen in the welding pools.

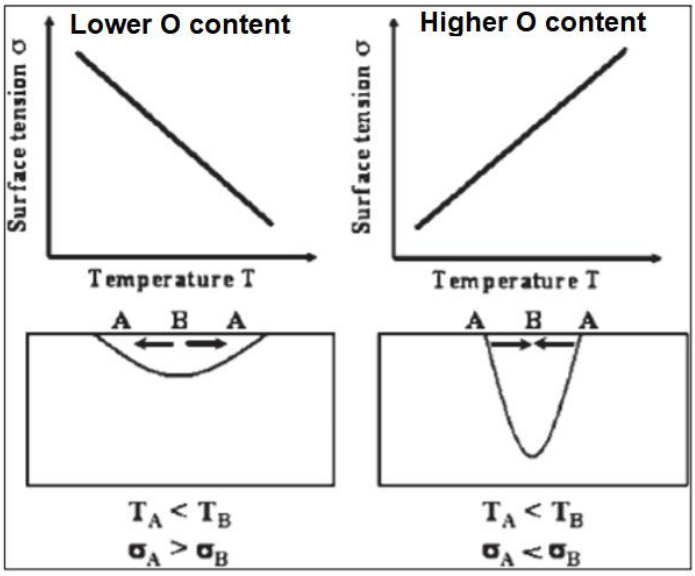

Fig.9: Model suggesting the increasing of penetration and decreasing of the bead width as a function of the oxygen content of the welding pool in "bead on plate" deposit through GTAW.

Figure 10 presents the groove test coupons welded with and without purging gas.

https://dx.doi.org/10.22161/ijaers.78.15 *ISSN: 2349-6495(P) | 2456-1908(O)*

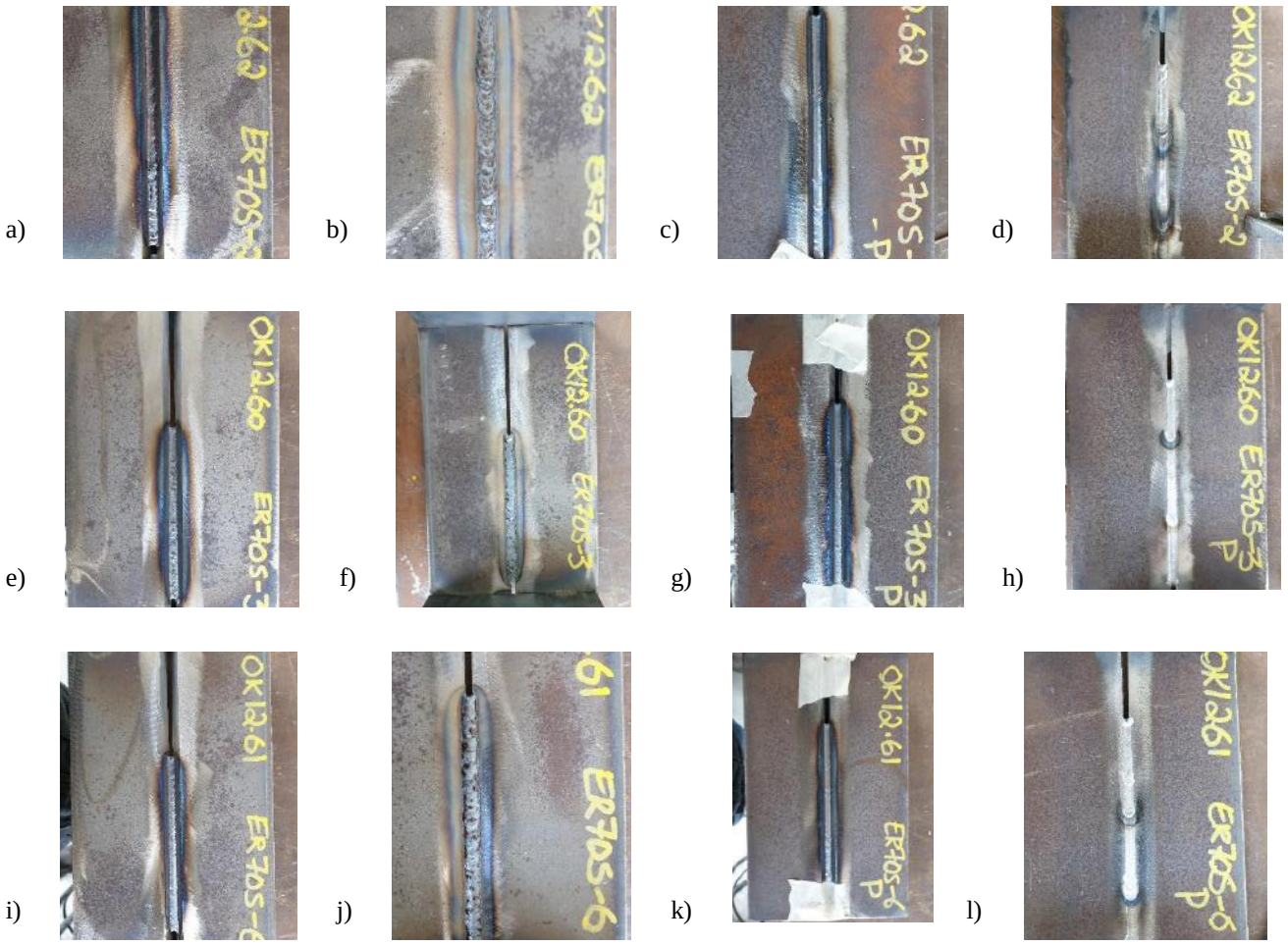

Fig.10: Groove test coupons welded with and without purging gas:
a) ER70S-2 – Face (no purging), b) ER70S-2 – Root (no purging), c) ER70S-2 – Face (purging),
d) ER70S-2 – Root (purging), e) ER70S-3 – Face (no purging), f) ER70S-3 – Root (no purging),
g) ER70S-3 – Face (purging), h) ER70S-3 – Root (purging), i) ER70S-6 – Face (no purging),
j) ER70S-6 – Root (no purging), k) ER70S-6 – Face (purging) and l) ER70S-6 – Root (purging)

The groove tests showed that both ER70S-2 and ER70S-6 presented weak weldability and ER70S-3 presented somewhat acceptable weldability without purging gas.

Using purging gas, all the filler metals presented very good weldability.

IV. CONCLUSIONS

Although the mechanical properties of the all weld metals produced using ER70S-2, ER70S-3 and ER70S-6 welding electrodes are quite similar, their chemical compositions are different specially in the contents of deoxidant elements like Zr, Al, Ti, Si and Mn.

The contents of deoxidizing elements are lower in ER70S-3, intermediate in ER70S-6 and higher in ER70S-2.

Deoxidized weld pools tend to have a negative temperature coefficient of surface tension. When the area under the arc is heated up, the surface tension drops in the center of the weld pool and the direction of the fluid flow is from the center towards the edges of the pool.

When oxygen, or other surface-active elements, are introduced to the weld pool at very low levels they cause the surface tension to rise with an increase in temperature. In this case, the direction of fluid flow is from the outside of the pool, where the surface tension is lower, towards the center, thus increasing penetration.

The choice of ER70S-2, ER70S-3 or ER70S-6 can lead to change in the direction of fluid flow in the welding pool due to change in the level of oxygen dissolved in the

https://dx.doi.org/10.22161/ijaers.78.15 *ISSN: 2349-6495(P) | 2456-1908(O)*

molten metal, resulting in changing in penetration and bead shape using the same welding parameters.

Welding of groove welds using ER70S-2 and ER70S-6 must be performed with purging gas.

REFERENCES

[1] Vicente, A. A.. **Estudo da resistência à oxidação ao ar a altas temperaturas de um aço inoxidável austenítico microligado ao cério soldado pelo processo mig/mag com diferentes gases de proteção.** Tese de Doutorado, Escola Politécnica, Universidade de São Paulo, São Paulo. 2017. https://doi:10.11606/t.3.2017.tde-05092017-103140.

[2] A. de Albuquerque Vicente, J.R.S. Moreno, D.C.R. Espinosa,T.F. de Abreu Santos, J.A.S. Tenório. **Study of the high temperature oxidation and Kirkendall porosity in dissimilar welding joints between FE-CR-AL alloy and stainless steel AISI 310 after isothermal heat treatment at 1150 °C in air.** J. Mater. Res. Technol. 8(2), 1636 (2019).https://doi.org/10.1016/j.jmrt.2018.11.009.

[3] Vicente, A. A.; Cabral, D. A.; Espinosa, D. C. R.; Tenório, J. A. S.. **Efeito dos gases de proteção na microestrutura e nas cinéticas de oxidação a altas temperaturas ao ar de juntas soldadas de um aço inoxidável austenítico através do processo MIG/MAG.** Tecnol. Metal. Mater. Min., vol.14, n4, p.357-365, 2017. https://doi.org/10.4322/2176-1523.1264.

[4] A.A. Vicente, J.R.S. Moreno, T.F.A. Santos, D.C.R. Espinosa, J.A.S. Tenório, **Nucleation and growth of graphite particles in ductile cast iron.** Journal of Alloys and Compounds, 775, pp. 1230-1234 (2019).https://doi.org/10.1016/j.jallcom.2018.10.136.

[5] VICENTE, A. A.; MORENO, J. R. S. ; TENÓRIO, J. A. S.; JUNIOR, A. B. B.; SANTOS, T. F. A.; ESPINOSA, D. C. R.. **Comparison of Behaviour to Oxidation at High Temperature of Two Superalloys: Inconel 713C and IC-50.** OXIDATION COMMUNICATIONS, v. 41, p. 195-204, 2018.

[6] Vicente, A. A.. **Oxidação ao ar a altas temperaturas de ligas à base de níquel.** Dissertação de Mestrado, Escola Politécnica, Universidade de São Paulo, São Paulo. 1999.https://doi:10.13140/RG.2.2.19144.88326

[7] JONES, D.A..**Atmospheric Corrosion and Elevated Temperature Oxidation. Principles and Prevention of Corrosion.** 2a Ed., Macmillan Ed., p.398-436, 1992.

[8] RIPOSAN, I., CHISAMERA, M., STAN, S., et al. **A New Approach to Graphite Nucleation Mechanism in Gray Irons.** In: Proceedings of the AFS Cast Iron Inoculation Conference, pp. 31-42, 2005.

[9] Lancaster, J. F., (1993). **Metallurgy of Welding.** 5th Edition, London. Chapman and Hall, p389.

[10] Kou, S.;Wang, Y. H.. **Weld pool convection and its effect.** Welding Journal. 65, p. 63-70, 1986.

[11] Mills K. C., Keene B. J., Brooks R. F. and ShiraliA..**Marangoni effects in welding**. Philosophical Transactionsof the Royal Society A.356. p. 911–925. 1998. http://doi.org/10.1098/rsta.1998.0196.

[12] Ahsan, M.R.U., Cheepu, M., Ashiri, R. et al. **Mechanisms of weld pool flow and slag formation location in cold metal transfer (CMT) gas metal arc welding (GMAW).** Weld World 61, p. 1275–1285 (2017). https://doi.org/10.1007/s40194-017-0489-y.

[13] Unni, A. K.;Vasudevan, M.. **Numerical modelling of fluid flow and weld penetration in activated TIG.** Materials Today: Proceedings. ISSN: 2214-7853. V. 27, p. 2768-2773 (2020). https://doi.org/10.1016/j.matpr.2019.12.196.

[14] ASTM E1086-08: Standard Test Method for Optical Emission Vacuum Spectrometric Analysis of Stainless Steel by the Point-to-Plane Excitation Technique. ASTM International. West Conshohocken. PA. EUA. 2008.